Li, X.; Kind, R.; Yuan, X.; Wölbern, I.; Hanka, W. Rejuvenation of the lithosphere by the Hawaiian plume In: Nature, 427, 6977 10.1038/nature02349 2004. 827-829 p.

Pacific[10] suggests that the bottom water in the western North Pacific is fed from the Samoa passage, spreading northwards through the Wake Island passage (see Fig. 1). In the South Pacific, the source region of the bottom water in the North Pacific, warming of the NADW has previously been suggested[7,11], all reporting changes in water masses in the Samoa passage, within the relatively recent time period when data are available.

These suggest that there is significant variability in the supply of Antarctic Bottom Water. Another recent study[12] concluded that mid-depth Southern Ocean temperatures have warmed by as much as 0.17 °C since the 1950s, when the modern accumulation of hydrographic data in this area started, within the Antarctic Circumpolar Current. This warming, together with the warming trend of the global ocean[1] is naturally expected to affect the Antarctic overturning system. It is interesting to speculate whether or not the changes we observe are directly related to the changes being observed in the South Pacific, and this will presumably be answered only after further revisits of WHP lines in the Pacific Ocean. □

Methods

The 1999 surveys all used SeaBird 911 CTD systems and field calibrations were completed using Guildline salinometers. The temperature sensors on the Japanese systems were calibrated within a month before and after each cruise and the accuracy of the temperature measurement is known to be better than 0.0007 °C. The temperature sensor on the Canadian system was calibrated three weeks before the survey to 0.0006 °C. Salinity observations were corrected using the standard seawater batch correction. This involved corrections of −0.0014 and −0.0015 to the Japanese observations, and −0.0009 to the Canadian data. We note that the separate segments of the survey did not match in the deep water until these corrections were made. Before differences were computed between the 1985 and 1999 surveys we converted the 1985 temperature observations from the reported values in the IPTS68 temperature scale to ITS90 (ref. 13), and applied the standard seawater batch correction[14–16], correcting salinities by +0.0012.

Received 22 July; accepted 31 December 2003; doi:10.1038/nature02337.

1. Levitus, S., Antonov, J. I., Boyer, T. P. & Stephens, C. Warming of the world ocean. *Science* **287,** 2225–2229 (2000).
2. Wong, A. P., Bindoff, N. L. & Church, J. A. Large–scale freshening of intermediate waters in the Pacific and Indian Oceans. *Nature* **400,** 440–443 (1999).
3. Roemmich, D. & Wunsch, C. Apparent changes in the climatic state of the deep North Atlantic Ocean. *Nature* **307,** 447–450 (1984).
4. Talley, L. D., Martin, M., Salameh, P. & the Oceanographic Data Facility. *Transpacific Section in the Subpolar Gyre (TPS47): Physical, Chemical, and CTD Data, R/V Thomas Thompson TT190, 4 August 1985–7 September 1985* 1–246 (Ref. 88–9, Scripps Inst. Of Oceanography, La Jolla, CA, 1988).
5. Talley, L. D., Joyce, T. & deSzoeke, R. A. Trans-Pacific sections at 47°N and 152°W: distribution of properties. *Deep-Sea Res. (Suppl.)* **38,** S63–S82 (1991).
6. Uchida, H., Fukasawa, M. & Freeland, H. J. *WHP P01 Revisit Data Book* 1–73 (Jamstec, Yokosuka, 2002).
7. Johnson, G. C., Rudnick, D. L. & Taft, B. A. Bottom water variability in the Samoa Passage. *J. Mar. Res.* **52,** 177–195 (1994).
8. Sclater, J. G. & Parsons, B. Oceans and continents: similarities and differences in the mechanisms of heat loss. *J. Geophys. Res.* **85,** 11535–11552 (1981).
9. Joyce, T. M., Warren, B. A. & Talley, L. D. The geothermal heating of the abyssal subarctic Pacific Ocean. *Deep-Sea Res.* **33,** 1003–1005 (1986).
10. Mantyla, A. & Reid, J. L. Abyssal characteristics of the world ocean waters. *Deep-Sea Res.* **30,** 805–833 (1983).
11. Johnson, G. C. & Orsi, A. H. Southwest Pacific water-mass exchanges between 1968/69 and 1990/91. *J. Clim.* **10,** 306–316 (1997).
12. Gille, S. H. Warming of the southern ocean since the 1950s. *Science* **295,** 1275–1277 (2002).
13. Preston-Thomas, H. The international temperature scale of 1990. *Metrologia* **27,** 3–10 (1990).
14. Mantyla, A. W. Standard seawater comparison updated. *J. Phys. Oceanogr.* **17,** 543–548 (1987).
15. Aoyama, M., Joyce, T., Kawano, T. & Takatsuki, Y. Standard seawater comparison up to P129. *Deep-Sea Res.* **49,** 1103–1114 (2002).
16. Kawano, T., Takatsuki, Y., Imai, J. & Aoyama, M. Seawater and quality evaluation of the standard seawater supplied in a bottle. [In Japanese with English abstract]. *J. Jpn Soc. Mar. Surv. Tech.* **13,** 11–18 (2001).
17. Reid, J. L. On the total geostrophic circulation of the Pacific Ocean: flow patterns, tracers and transports. *Prog. Oceanogr.* **39,** 263–352 (1997).

Acknowledgements We thank the officers and crew of the three research vessels (RV *Kaiyo-maru* of JFA, RV *Mirai* of JAMSTEC, and CCGS *John P. Tully*) and all technical assistants. The Canadian contribution was funded by the Strategic Science Fund of the Department of Fisheries and Oceans, and the Japanese contributions were funded by the Promotional Foundation for Science and Technology of the Science and Technology Agency of Japan (now known as the Ministry of Education, Culture, Sports, Science and Technology).

Competing interests statement The authors declare that they have no competing financial interests.

Correspondence and requests for materials should be addressed to M.F. (fksw@jamstec.go.jp) or H.F. (FreelandHj@pac.dfo-mpo.gc.ca).

Rejuvenation of the lithosphere by the Hawaiian plume

Xueqing Li[1], Rainer Kind[1,2], Xiaohui Yuan[1], Ingo Wölbern[1] & Winfried Hanka[1]

[1]*GeoForschungsZentrum Potsdam, Telegrafenberg, 14473 Potsdam, Germany*
[2]*Freie Universität Berlin, FR Geophysik, Malteserstrasse 74–100, 12249 Berlin, Germany*

The volcanism responsible for creating the chain of the Hawaiian islands and seamounts is believed to mark the passage of the oceanic lithosphere over a mantle plume[1,2]. In this picture hot material rises from great depth within a fixed narrow conduit to the surface, penetrating the moving lithosphere[3]. Although a number of models describe possible plume–lithosphere interactions[4], seismic imaging techniques have not had sufficient resolution to distinguish between them. Here we apply the S-wave 'receiver function' technique to data of three permanent seismic broadband stations on the Hawaiian islands, to map the thickness of the underlying lithosphere. We find that under Big Island the lithosphere is 100–110 km thick, as expected for an oceanic plate 90–100 million years old that is not modified by a plume. But the lithosphere thins gradually along the island chain to about 50–60 km below Kauai. The width of the thinning is about 300 km. In this zone, well within the larger-scale topographic swell, we infer that the rejuvenation model[5] (where the plume thins the lithosphere) is operative; however, the larger-scale topographic swell is probably supported dynamically.

Thermomechanical processes caused by plume–lithosphere interactions have been studied for several decades. Various models have been proposed to explain the generating mechanism of the Hawaiian swell: (1) a model in which the dynamic pressure of the plume material flowing in the asthenosphere away from the plume centre supports the uplift of the sea floor[4,6]; (2) the thermal resetting (rejuvenation) model, in which the oceanic lithosphere is heated when it passes the hotspot, and thinning of the lithosphere causes isostatic uplift of the Hawaiian swell[5]; (3) a model in which

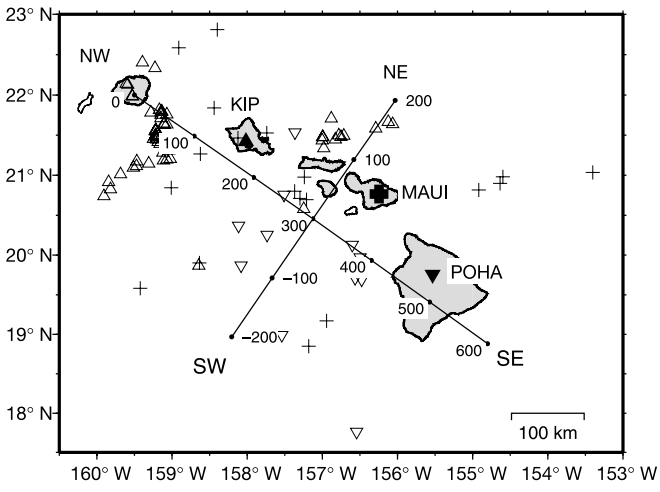

Figure 1 Location map of permanent broadband stations KIP (IRIS/GEOSCOPE), MAUI (GEOFON) and POHA (IRIS/USGS). Piercing points of S-receiver functions at 100 km depth are shown (same symbols as stations). Two lines labelled NW–SE and SW–NE indicate the two sections shown in Fig. 2 onto which the S-receiver functions are projected. Section NW–SE is along the island chain while section SW–NE is perpendicular to the chain.

extracted basaltic melt of the plume material underplates the base of the lithosphere. This residue of the plume material is compositionally lighter and has high seismic velocity[7–9]. Different models predict different seismic thicknesses of the lithosphere. In the first model, the lithospheric thickness along the swell is relatively stable. The second model (thermal rejuvenation) predicts a thinner lithosphere when it passes the hotspot. The lithospheric thickness in the third model will be larger than normal.

Until now, only the following observations of the lithospheric thickness by means of different seismic data have been available. In studies of surface-wave dispersion between Big Island and Oahu, a thickness of 88 km was suggested for a lithosphere 80–90 million years (Myr) old[10]. Between Oahu and Midway, 2,000 km northwest of Oahu, the average lithospheric thickness is estimated to be 100 km for a 50–110-Myr-old lithosphere[11,12]. In studies using converted waves, the thickness beneath Oahu was suggested to be 65–80 km (refs 13, 14), and 80 km southwest of Oahu[15]. From surface-wave dispersion data of an OBS (ocean bottom seismometer) array southwest of Oahu and Big Island, the average seismic structure of a 100-Myr-old oceanic lithosphere was derived and a significant velocity reduction at asthenospheric depths closer than 300 km to the island chain was found[16]. These facts are not sufficient to distinguish between competing models of lithosphere–plume interaction.

We have applied seismic techniques (S-receiver functions[13,17,18]) developed for P-receiver function studies to S-to-P converted waves (see Supplementary Information for a comparison of both techniques). S-receiver functions have been calculated from data of the permanent broadband stations POHA (IRIS/USGS), MAUI (GEOFON/ GeoForschungsZentrum, Potsdam) and KIP (IRIS/ GEOSCOPE), which are located on the islands of Hawaii, Maui and Oahu, respectively. The locations of the stations POHA, MAUI and KIP and the piercing points of the S-to-P conversions at 100 km depth are shown in Fig. 1. Figure 2 shows the stacked S-receiver functions for a section NW–SE along the island chain (Fig. 2a) and a section SW–NE perpendicular to it (Fig. 2b). The sections are formed by stacking individual traces with piercing points at depths of 100 km within a window of length 30 km. Then the window is moved by 20 km for a new summation trace. Before summation, all traces were corrected for epicentral distance or slowness. A reference slowness of 6.4 s deg^{-1} has been chosen, similar to that in many P-receiver function studies, making P-to-S and S-to-P differential times directly comparable.

To suppress oceanic noise, a 7–20 s bandpass filter is applied. We reversed the polarity of amplitudes to compare the data directly with P-receiver functions. A clear negative phase (LAB, lithosphere–asthenosphere boundary) is identified in Fig. 2a, b. Negative (shaded) amplitudes are caused by velocity reduction downwards. To confirm that this phase is caused by the LAB, we compared the S-receiver functions with conventional P-receiver functions at the same stations and found good agreements (see Supplementary Information). The data in Fig. 2 are in the time domain. These delay times (in seconds) can roughly be converted into depth (in kilometres) by multiplying all times with a factor of 9, from the IASP91 model.

Figure 2a shows clearly that along the island chain the LAB thins from Big Island (12 s or 108 km depth at profile kilometre 500) to Kauai (6 s or 54 km depth at profile kilometre 0). Perpendicular to the island chain on the SW–NE section (Fig. 2b), the LAB is at 12 s delay time (108 km deep) at profile kilometres −150 to −100 and again at profile kilometre 200, northeast of the chain. It thins to 7–8 s (63–72 km deep) at profile kilometres 50–100 which is directly beneath the island chain along the profile (Fig. 1). The NW–SE section (Fig. 2a) contains all available S-to-P data. The perpendicular SW–NE section (Fig. 2b) contains only records with piercing points southeast of Oahu, which have similar minimum LAB depths. The two profiles in Fig. 2 indicate thinning of the lithosphere from Big Island to Oahu and Kauai as imaged in Fig. 3. The end of the thinning in the northwest direction is not visible. A station on Kauai or OBS stations northwest of Kauai would be necessary to follow the continuation of the lithospheric thinning.

We obtain from our observations the following picture of the plume–lithosphere interaction. Whereas the Pacific plate overrides the Hawaiian plume with a velocity of 7–8 cm yr^{-1}, plume material hits the lithosphere and is dragged off. It spreads mainly in the direction of the plate motion and causes a long tail along the Hawaiian island chain. The bottom of the lithosphere is heated by

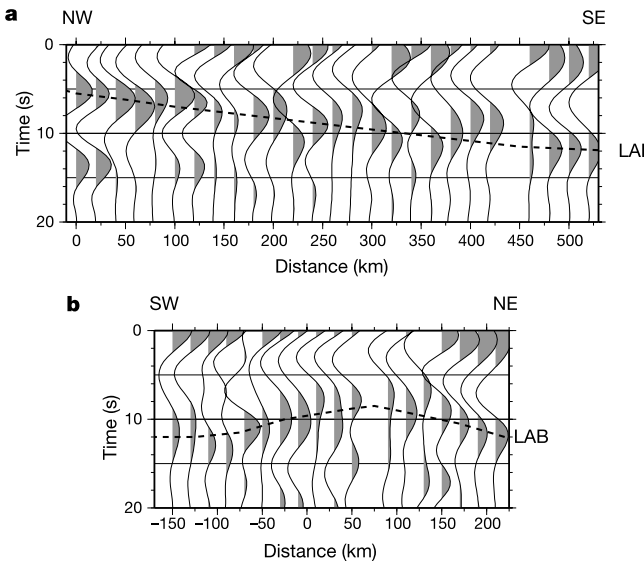

Figure 2 Stacked S-receiver functions of the three stations projected on the two profiles of Fig. 1 according to their piercing points at 100 km depth. **a**, Along the island chain (NW–SE); **b**, perpendicular to it (SW–NE). Zero time corresponds to the S-wave arrival. The timescale is reversed. The stack bin is 30 km with 10 km overlap. Slowness (or distance) move-out corrections are applied (reference slowness of 6.4 s deg^{-1}) before stacking. In section NW–SE (**a**) all S-to-P data are used that cover an up to 200-km broad sampling region at 100 km depth on each side of the section. In section SW–NE (**b**) only S–P data southeast of KIP (Oahu) are used. A 7–20 s bandpass filter is applied to suppress the noise. LAB indicates the lithosphere–asthenosphere boundary, which is a precursor of the S wave.

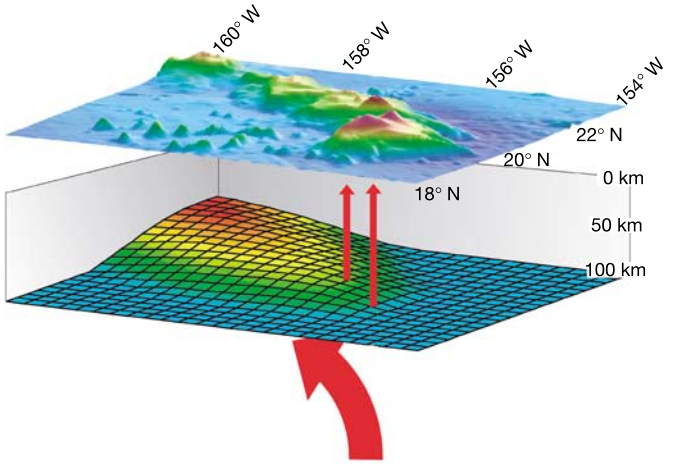

Figure 3 Sketch of the obtained lithosphere–asthenosphere boundary below the Hawaiian island chain.

the plume material from below and the increased temperature will reduce the velocity of elastic waves. In the vicinity of the present plume centre, only the lowest part of the lithosphere is heated and the lithospheric thickness does not change much with respect to that of a 90–100-Myr-old oceanic plate. As time increases, more and more material from the lower part of the lithosphere is warmed up and the seismic LAB becomes shallower. After 3–4 Myr of heating time the thinnest lithosphere of 50–60 km is achieved beneath Oahu and Kauai—a location about 400 km away from the current plume centre[10]. Further away, at Midway Island, which passed the plume centre about 28 Myr ago, the plume material begins to lose its temperature and the lithosphere thickens again[11,12].

We conclude that the Hawaiian plume has gradually reheated up to 50 km of the lower lithosphere within the last 3–4 Myr in an area of 500 × 300 km along the island chain. This means that a substantial amount of heat is trapped below the lithosphere. The lateral extent of the asthenospheric updoming is significantly smaller than the extent of the Hawaiian topographic swell. A consequence of our result could be that the entire topographic swell is caused by, for example, the dynamic support of the plume, and so rejuvenation would be contributing only in the central part. Data from longer-term broadband stations on Kauai, and on the ocean bottom northwest of Kauai, could permit imaging of the 're-ageing' of the rejuvenated Hawaiian lithosphere. □

Received 27 September 2003; accepted 14 January 2004; doi:10.1038/nature02349.

1. Wilson, J. T. A possible origin of the Hawaiian island. *Can. J. Phys.* **41,** 863–868 (1963).
2. Morgan, W. J. Convective plumes in the lower mantle. *Nature* **230,** 42–43 (1971).
3. Nataf, H.-C. Seismic imaging of mantle plumes. *Annu. Rev. Earth Planet. Sci.* **28,** 391–417 (2000).
4. Ribe, N. M. & Christensen, U. R. The dynamical origin of the Hawaiian volcanism. *Earth Planet. Sci. Lett.* **171,** 517–531 (1999).
5. Detrick, R. S. & Crough, S. T. Island subsidence, hot spots, and lithospheric thinning. *J. Geophys. Res.* **83,** 1236–1244 (1978).
6. Sleep, N. H. Hotspots and mantle plumes: Some phenomenology. *J. Geophys. Res.* **95,** 6715–6736 (1990).
7. Jordan, T. H. in *The Mantle Sample: Inclusions in Kimberlites and Other Volcanics* (eds Boyd, F. R. & Meyer, H. O. A.) 1–14 (Proc. 2nd Int. Kimberlite Conference, American Geophysical Union, 1979).
8. Robinson, E. M. The topographic and gravitational expression of density anomalies due to melt extraction in the uppermost oceanic mantle. *Earth Planet. Sci. Lett.* **90,** 221–228 (1988).
9. Phipps Morgan, J., Morgan, W. J., Zhang, Y.-S. & Smith, W. H. F. Observational hints for a plume-fed, suboceanic asthenosphere and its role in mantle convection. *J. Geophys. Res.* **100,** 12753–12767 (1995).
10. Priestley, K. & Tilmann, F. Shear-wave structure of the lithosphere above the Hawaiian hot spot from two-station rayleigh wave phase velocity measurements. *Geophys. Res. Lett.* **26,** 1493–1496 (1999).
11. Woods, M., Leveque, J. J. & Okal, E. A. Two-station measurements of Rayleigh wave group velocity along the Hawaiian swell. *Geophys. Res. Lett.* **18,** 105–108 (1991).
12. Woods, M. T. & Okal, E. A. Rayleigh-wave dispersion along the Hawaiian Swell: a test of lithospheric thinning by the thermal rejuvenation at a hotspot. *Geophys. J. Int.* **125,** 325–339 (1996).
13. Bock, G. Long-period S to P converted waves and the onset of partial melting beneath Oahu, Hawaii. *Geophys. Res. Lett.* **18,** 869–872 (1991).
14. Li, X. *et al.* Mapping the Hawaiian plume with converted seismic waves. *Nature* **405,** 938–941 (2000).
15. Collins, J. A., Vernon, F. L., Orcutt, J. A. & Stephen, R. A. Upper mantle structure beneath the Hawaiian swell: constraints from the ocean seismic network pilot experiment. *Geophys. Res. Lett.* **29,** doi: 101029/2001GL013302 (2002).
16. Laske, G., Phipps Morgan, J. & Orcutt, J. A. First results from the Hawaiian SWELL pilot experiment. *Geophys. Res. Lett.* **26,** 3397–3400 (1999).
17. Faber, S. & Müller, G. Sp phases from the transition zone between the upper and lower mantle. *Bull. Seismol. Soc. Am.* **70,** 487–508 (1980).
18. Farra, V. & Vinnik, L. Upper mantle stratification by P and S receiver functions. *Geophys. J. Int.* **141,** 699–712 (2000).

Supplementary Information accompanies the paper on **www.nature.com/nature**.

Acknowledgements We thank G. Asch and J. Mechie for their aid. We also thank the people of the Kaleahala National Park for supporting our station MAUI. This work has been supported by the Deutsche Forschungsgemeinschaft within the ICDP project and by the GeoForschungsZentrum, Potsdam. Waveform data have been provided by the IRIS, GEOSCOPE and GEOFON data centres.

Competing interests statement The authors declare that they have no competing financial interests.

Correspondence and requests for materials should be addressed to R.K. (kind@gfz-potsdam.de).

Iron corrosion by novel anaerobic microorganisms

Hang T. Dinh[1], Jan Kuever[1,2], Marc Mußmann[1], Achim W. Hassel[3], Martin Stratmann[3] & Friedrich Widdel[1]

[1]*Max Planck Institute for Marine Microbiology, Celsiusstraße 1, 28359 Bremen, Germany*
[2]*Institute for Material Testing, Paul-Feller-Straße 1, 28199 Bremen, Germany*
[3]*Max Planck Institute for Iron Research, Max-Planck-Straße 1, 40237 Düsseldorf, Germany*

Corrosion of iron presents a serious economic problem. Whereas aerobic corrosion is a chemical process[1], anaerobic corrosion is frequently linked to the activity of sulphate-reducing bacteria (SRB)[2–6]. SRB are supposed to act upon iron primarily by produced hydrogen sulphide as a corrosive agent[3,5,7] and by consumption of 'cathodic hydrogen' formed on iron in contact with water[2–6,8]. Among SRB, *Desulfovibrio* species—with their capacity to consume hydrogen effectively—are conventionally regarded as the main culprits of anaerobic corrosion[2–6,8–10]; however, the underlying mechanisms are complex and insufficiently understood. Here we describe novel marine, corrosive types of SRB obtained via an isolation approach with metallic iron as the only electron donor. In particular, a *Desulfobacterium*-like isolate reduced sulphate with metallic iron much faster than conventional hydrogen-scavenging *Desulfovibrio* species, suggesting that the novel surface-attached cell type obtained electrons from metallic iron in a more direct manner than via free hydrogen. Similarly, a newly isolated *Methanobacterium*-like archaeon produced methane with iron faster than do known hydrogen-using methanogens, again suggesting a more direct access to electrons from iron than via hydrogen consumption.

Some 10% of all corrosion damages to metals and non-metals may result from microbial activities[11]. A significant process in this respect is the anaerobic corrosion of iron or steel, for instance in oil technology[3,6,11]. The primary dissolution ($Fe \rightleftarrows Fe^{2+} + 2e^-$; $E^0 = -0.44\,V$) can in principle be driven by numerous oxidants. In oxic humid surroundings, oxidation by O_2 ($E^0_{pH7} = +0.82\,V$) yields rust[1]. In anoxic surroundings, H^+ ions from water yield H_2 ($E^0_{pH7} = -0.41\,V$). Of the sequential steps ($2e^- + 2H^+ \rightarrow 2H_{(adsorbed)} \rightarrow H_{2(adsorbed)} \rightarrow H_{2(aqueous)}$), the combination of the H atoms is presumably rate-limiting[12] and is a main reason for the slowness of iron oxidation in anoxic sterile water ($Fe + 2H_2O \rightarrow Fe^{2+} + H_2 + 2HO^-$). However, sulphate-reducing bacteria (SRB) promote the anaerobic oxidation of iron[2–6]. Their activity often occurs in biofilms and tends to pit the iron[2,3,13]. An indirect and a direct corrosion mechanism may be distinguished[3,5]: these may occur simultaneously at different extents, depending on the load of waters with biodegradable organic compounds.

The indirect mechanism is a chemical attack by hydrogen sulphide ($Fe + H_2S \rightarrow FeS + H_2$) which is faster than that by water[3,5,7] and also promotes so-called hydrogen embrittlement of the metal[1,12] (see also http://www.corrosion-doctors.org). Because SRB commonly use organic compounds (shown here as $[CH_2O]$) and often also H_2 for sulphate reduction, the net reaction of indirect corrosion (for complete carbon oxidation by SRB communities) can be written as:

$$2[CH_2O] + 1\tfrac{1}{3}Fe + 1\tfrac{1}{3}\,SO_4^{2-} + \tfrac{2}{3}H^+ \rightarrow 2HCO_3^- + 1\tfrac{1}{3}FeS + 1\tfrac{1}{3}H_2O \quad (1)$$

In the direct mechanism according to the depolarization theory (see Supplementary Information)[8], SRB are supposed to stimulate corrosion by scavenging 'cathodic hydrogen' or a 'hydrogen film'